Binding of Six Nucleotide Cofactors to the Hexameric Helicase RepA Protein of Plasmid RSF1010. 1. Direct Evidence of Cooperative Interactions between the Nucleotide-Binding Sites of a Hexameric Helicase†

Maria J. Jezewska, Aaron L. Lucius, and Wlodzimierz Bujalowski*

Department of Human Biological Chemistry and Genetics, Department of Obstetrics and Gynecology, the Sealy Center for Structural Biology, Sealy Center for Cancer Cell Biology, The University of Texas Medical Branch at Galveston, 301 University Boulevard, Galveston, Texas 77555-1053

Received September 10, 2004; Revised Manuscript Received December 15, 2004

ABSTRACT: The interactions of nucleotides with RepA hexameric helicase from plasmid RSF1010 have been examined using nucleotide analogues, TNP-ADP, TNP-ATP, and MANT-ADP. The binding of the analogues is accompanied by strong quenching of the protein fluorescence. A quantitative fluorescence titration method has been applied to analyze the interactions, independent of any assumptions of proportionality between the fluorescence quenching and the average degree of binding. The fluorescence quenching as a function of the average degree of binding is expressed by an empirical function that enables analysis of the data, without the necessity of determining quenching parameters for different complexes. At saturation, the RepA hexamer binds six nucleotide molecules, indicating that each subunit of the hexamer can engage in interactions with the cofactor. The nucleotide macroscopic affinity decreases with the increasing degree of binding, indicating heterogeneity among the binding sites. A statistical thermodynamic hexagon model provides an excellent description of the binding process and requires only two interaction parameters, the intrinsic binding constant, K, and cooperativity parameter, σ. The heterogeneity in affinity reflects negative cooperative interactions between the binding sites. Analyses of the data provide clear evidence that the alternative model of two independent classes of binding sites does not describe the nucleotide binding. Such a model cannot account for both, the binding isotherms and the dependence of the fluorescence quenching upon the degree of binding. Thus, cooperative interactions between the nucleotide-binding sites are an intrinsic property of the RepA helicase. The presence of the cooperative interactions indicates significant communication among the subunits of the helicase.

Unwinding of the duplex nucleic acid, to form transiently a metabolically active single-stranded intermediate, is catalyzed by a class of enzymes called helicases, in a reaction that is fueled by the hydrolysis of nucleoside triphosphates (*1*−*4*). Although some helicases can function as monomeric single peptide units, most often, the enzymes function as oligomeric structures containing two or more protomers that provide the enzyme with multiple active sites required in their motor protein activities (*2*, *5*−*9*). For instance, in the *Escherichia coli* cell, the primary replicative helicase, the DnaB protein, forms a stable ring-like hexamer, specifically stabilized by the binding of multiple magnesium cations (*5*, *6*). Other well-known replicative helicases, bacteriophage T7 and T4 enzymes, as well as the *E. coli* transcription termination factor Rho helicase, form hexameric ring-like structures that require or are stabilized by nucleotide cofactor and/or DNA binding (*7*−*9*).

The broad host nonconjugative plasmid RSF1010 confers bacterial resistance to sulfonamides and streptomycin (*10*, *11*). RSF1010 codes its own replicative helicase, the RepA protein. The RepA helicase unwinds the duplex DNA in the 5′ → 3′ direction and is essential for the RFS1010 plasmid replication in bacterial cells (*13*−*17*). As revealed by the crystallographic studies, the enzyme is a hexameric helicase with a ring-like structure and a central cross channel with a diameter of ∼17 Å (*14*). However, a puzzling aspect of the RepA helicase structure is its strong dependence on pH (*13*−*16*). The protein exists as a very stable hexamer at neutral pH, while at pH ≤ 6, the RepA helicase forms a dodecamer, i.e., a dimer of two hexamers, as seen in the crystal structure, although it is still unclear whether the dodecamer seen in the crystallographic studies corresponds to the dodecamer formed in solution (*14*).

As mentioned above, the unwinding of the duplex nucleic acid is a complex free-energy transduction process that requires binding and hydrolysis of nucleoside triphosphates (NTPs)[1] by a helicase (*2*−*4*). However, how the binding and/or hydrolysis of NTPs regulate the activity of the enzyme and its affinity toward nucleic acids is still minimally understood for any helicase, particularly, at the molecular

† This work was supported by NIH Grant R01 GM-46679 (to W.B.).

* To whom correspondence should be addressed: Department of Human Biological Chemistry and Genetics, The University of Texas Medical Branch at Galveston, 301 University Boulevard, Galveston, TX 77555-1053. Telephone: (409) 772-5634. Fax: (409) 772-1790. E-mail: wbujalow@utmb.edu.

[1] Abbreviations: TNP-ADP, 2′(3′)-*O*-(2,4,6-trinitrophenyl)adenosine-5′-diphosphate; TNP-ATP, 2′(3′)-*O*-(2,4,6-trinitrophenyl)adenosine; NTP, nucleoside triphosphate; Tris, tris(hydroxymethyl)aminomethane.

10.1021/bi048037+ CCC: $30.25
Published on Web 02/15/2005

level. The unwinding of the duplex DNA by the RepA protein has been found to be most efficient in the presence of ATP and GTP (*12*, *17*). Yet, hydrolysis of NTPs is not necessary for binding of RepA protein to the ssDNA. The enzyme can bind the ssDNA in the presence of nonhydrolyzable ATP analogues. In this context, the RepA hexamer resembles the behavior of the *E. coli* DnaB helicase (*19*−*28*). Moreover, both helicases form stable hexameric structures; nevertheless, while the DnaB hexamer requires magnesium to sustain the hexamer, the RepA protein hexamer does not require any specific cofactors to maintain its structure (*12*, *15*). Also, in contrast to the DnaB protein, the RepA helicase can utilize dNTP in the unwinding reaction, while the DnaB helicase does not show any dATPase activities.

It is clear that understanding the interactions of nucleotides with the RepA protein and their regulatory role is a key element for understanding the helicase activity of the enzyme; however, the mechanism and the character of this control remains obscure, particularly at the molecular level. Little is known about the nucleotide cofactor binding to the RepA hexamer, and the available data are only of semiquantitative nature (*17*) (see below). Such fundamental parameters of the interaction of the RepA hexamer with nucleotides, like the maximum stoichiometry of the protein−nucleotide complex, i.e., the maximum number of subunits of the hexamer that are able to actively engage in nucleotide binding, the nature of the binding process, intrinsic affinities of the nucleotide-binding sites, and cooperativity of the binding are still unknown.

Quantitative information about the interactions of the RepA helicase with nucleotide cofactors is a necessary prerequisite to formulate a model of the activity of the enzyme. Moreover, the functional and structural homology between the RepA and DnaB hexamer makes RepA protein an excellent system for comparative studies. In this context, elucidation of the RepA hexamer interactions with nucleotide cofactors is of paramount importance for understanding general aspects of hexameric helicase activities. On the other hand, the fact that the RepA helicase is essential for the RSF1010 plasmid replication suggests that the protein is involved in specific mechanisms during the DNA replication, not yet known. The essential role of the helicase in replication of the RSF1010, a ubiquitous multiple copy plasmid, conferring resistance to antibiotics, provides an opportunity to examine molecular aspects of such resistance (*10*, *11*).

In this paper, we present direct quantitative evidence that there are six nucleotide-binding sites on the RSF1010 RepA hexamer that differ significantly in their affinities for the nucleotides. Moreover, the observed heterogeneity in the macroscopic affinity results from the negative cooperative interactions between the binding sites. A statistical thermodynamic model, the hexagon model, provides an excellent description of the binding isotherms using only two interaction parameters. The application of the model enables us to extract the contributions of both the intrinsic affinity and negative cooperativity to the overall binding process. Analyses of the experimental data show that an alternative model of two independent classes of independent binding sites does not describe the nucleotide binding to the RepA hexamer.

MATERIALS AND METHODS

Reagents and Buffers. All chemicals were reagent-grade. All solutions were made with distilled and deionized >18 MΩ (Milli-Q Plus) water. Buffer T5 is 50 mM tris(hydroxymethyl)aminomethane (Tris) adjusted to pH 7.6 with HCl and 10% glycerol. The temperature and concentration of NaCl and $MgCl_2$ in the buffer are indicated in the text.

RepA Helicase of Plasmid RSF1010. The gene of the RepA helicase has been isolated directly from plasmid RSF1010 and placed in plasmid pET30a under control of the T7 polymerase system. Isolation and purification of the protein was performed, with slight modifications, as described (*12*). The protein was >99% pure as judged by sodium dodecyl sulfate−polyacrylamide gel electrophoresis with Coomasie Brilliant Blue staining. The concentration of the protein was spectrophotometrically determined using the extinction coefficient $\epsilon_{280} = 1.66 \times 10^5\ cm^{-1}\ M^{-1}$, obtained with the approach based on Edelhoch's method (*29*, *30*).

Nucleotides. 2′(3′)-*O*-(2,4,6-Trinitrophenyl)adenosine (TNP-ATP) and 2′(3′)-*O*-(2,4,6-trinitrophenyl)adenosine-5′-diphosphate (TNP-ADP) were from Molecular Probes (Eugene, OR). MANT-ADP was synthesized as previously described (*31*). All nucleotides used in the binding studies were >95% pure as judged by TLC on silica.

Fluorescence Measurements. All steady-state fluorescence titrations were performed using the SLM-AMINCO 8100C. To avoid possible artifacts, because of the fluorescence anisotropy of the sample, polarizers were placed in excitation and emission channels and set at 90° and 55° (magic angle), respectively (*32*, *33*). The cofactor binding was followed by monitoring the fluorescence of the RepA helicase ($\lambda_{ex} = 300$ nm and $\lambda_{em} = 340$ nm). Computer fits were performed using Mathematica (Wolfram, IL) and KaleidaGraph (Synergy Software, PA). All titration points were corrected for dilution and inner-filter effects using the following formula (*25*)

$$F_{icor} = (F_i - B_i)\left(\frac{V_i}{V_o}\right)10^{0.5b(A_{i\lambda ex}+A_{i\lambda em})} \qquad (1)$$

where F_{icor} is the corrected value of the fluorescence intensity at a given point of titration, F_i is the experimentally measured fluorescence intensity, B_i is the background, V_i is the volume of the sample at a given titration point, V_o is the initial volume of the sample, b is the total length of the optical path of the sample expressed in centimeters, and $A_{i\lambda ex}$ and $A_{i\lambda em}$ are the absorbances of the sample at excitation and emission wavelengths, respectively (*25*). The RepA protein relative fluorescence quenching, ΔF_{obs}, upon binding a nucleotide cofactor is defined as $\Delta F_{obs} = (F_o - F_{icor})/F_o$, where F_i is the fluorescence of the nucleic acid at a given titration point and F_o is the initial value of the fluorescence of the sample (*25*).

Quantitative Determination of Binding Isotherms and Stoichiometries of the RepA Hexamer−Nucleotide Cofactor Complexes. In this work, we followed the binding of nucleotide cofactors to the RepA helicase by monitoring the fluorescence quenching, ΔF_{obs}, of the protein emission upon the complex formation. A rigorous method to estimate the average degree of binding, $\sum\Theta_i$ (number of nucleotide molecules bound per RepA hexamer), and the free nucleotide concentration, P_F, has been previously described in detail

by us (*34*−*36*). Briefly, the experimentally observed ΔF_{obs} has a contribution from each of the different possible "i" complexes of the RepA hexamer with the cofactor. Thus, the observed fluorescence quenching is functionally related to $\sum\Theta_i$ by

$$\Delta F_{obs} = \sum \Theta_i \Delta F_{i_{max}} \quad (2)$$

where $\Delta F_{i_{max}}$ is the molecular parameter characterizing the molar fluorescence quenching of the RepA helicase with the nucleotide cofactor bound in complex "i". The same value of ΔF_{obs}, obtained at two different total helicase concentrations, P_{T_1} and P_{T_2}, indicates that the same physical state of the hexamer, i.e., the degree of binding, $\sum\Theta_i$, and the free nucleotide concentration, N_F, must be the same. The values of $\sum\Theta_i$ and N_F are then related to the total nucleotide concentrations, N_{T_1} and N_{T_2}, and the total protein concentrations, P_{T_1} and P_{T_2}, at the same value of ΔF_{obs}, by

$$\sum \Theta_i = \frac{N_{T_2} - N_{T_1}}{P_{T_2} - P_{T_1}} \quad (3a)$$

$$N_F = N_{T_x} - (\sum \Theta_i) P_{T_x} \quad (3b)$$

where $x = 1$ or 2 (*34*−*36*).

Empirical Function Method. The data discussed below show that the RepA hexamer has six nucleotide-binding sites and each enzyme−nucleotide complex can exist in multiple conformational states characterized by different molar fluorescence intensities. Thus, it is practically impossible to obtain independently all optical parameters for different complexes to fit the experimental fluorescence titration curves (*25*, *35*). However, this problem can be solved by introducing the representation of the observed quenching of the protein fluorescence, ΔF_{obs}, upon the binding of the nucleotides, as a function of the average degree of binding, $\sum\Theta_i$, via an empirical function (*25*, *35*). The approach makes possible the analysis of a single experimental titration curve without the necessity of determining all fluorescence parameters for different complexes. An empirical function is used, usually a polynomial, that accurately relates the experimentally determined dependence of the spectroscopic parameter (in our case, fluorescence quenching, ΔF_{obs}) to the average degree of binding, $\sum\Theta_i$, defined as

$$\Delta F_{obs} = \sum_{j=0}^{n} a_j (\sum \Theta_i)^j \quad (4)$$

where a_j values are the fitting constants. This function is then used to generate a theoretical isotherm for a binding model and to extract intrinsic binding parameters for a particular binding model, from the experimentally obtained single titration curve (see below).

The value of the degree of binding, $\sum\Theta_i$, is calculated for a given free nucleotide concentration and initial estimates of intrinsic binding parameters. The obtained $\sum\Theta_i$ is then introduced into eq 4, and the value of ΔF_{obs}, corresponding to a given value of $\sum\Theta_i$, is calculated. These calculations are then performed for the entire titration curve (*25*, *35*). It should be noted that it is necessary to apply the procedure to a binding system to establish the relationship between ΔF_{obs} and $\sum\Theta_i$ and to verify that it is true over the range of studied solution conditions. The method can be used for any ligand−macromolecule system, where the determination of all molecular constants in an analytical equation is practically impossible (*25*, *35*).

RESULTS

Quantitative Determination of Stoichiometries of the Nucleotide Cofactor−*RSF1010 RepA Hexamer Complex.* Binding of the unmodified nucleotide cofactors to the RepA hexamer is not accompanied by a change of the protein fluorescence that is adequate to perform quantitative analysis of the complex binding process. However, we found that binding of nucleotide analogues, TNP-ATP and TNP-ADP, to the RepA protein is accompanied by a strong quenching of the protein fluorescence, providing an excellent signal to monitor the association. The hydrolysis of TNP-ATP is undetectable on the time scale of the binding experiments (accompanying paper 2).

Fluorescence titrations of the RepA hexamer with TNP-ADP, at three different protein concentrations, in buffer T5 (at pH 7.6 and 10 °C), containing 10 mM NaCl and 1 mM $MgCl_2$, are shown in Figure 1a. The maximum quenching of the protein fluorescence at saturation is 0.87 ± 0.03. The selected protein concentrations provide the separation of the binding isotherms up to the quenching value of ∼0.83. As pointed out above, the RepA protein exists, in the examined solution conditions, as a very stable hexamer and does not require any specific cofactors to maintain its structure (*12*, *15*). The stability of the RepA hexamer has been recently confirmed using the analytical centrifugation method (*36*). The spectroscopic titration curves in Figure 1a would indicate an apparent single binding process. However, analysis of the data, using the approach outlined in the Materials and Methods, reveals a more complex behavior (*25*, *35*). To obtain a thermodynamically rigorous binding isotherm, independent of any assumption about the relationship between the observed signal and the degree of binding, $\sum\Theta_i$, the titration curves, shown in Figure 1a, have been analyzed, using the method outlined in the Materials and Methods (*34*, *37*).

The dependence of the observed fluorescence quenching, ΔF_{obs}, upon the average degree of binding, $\sum\Theta_i$, of the TNP-ADP on the RepA hexamer is shown in Figure 1b. The separation of the binding isotherms allows us to obtained the values of $\sum\Theta_i$ up to ∼5.1 of the TNP-ADP molecules per RepA hexamer. The plot in Figure 1b is clearly nonlinear. For comparison, the dashed line represents the hypothetical case when a strict proportionality between the degree of cofactor binding and the quenching of the RepA hexamer fluorescence would exist. Thus, binding of the first three molecules of the nucleotide induces a larger decrease of the protein fluorescence emission than the binding of the subsequent cofactor molecules. Short extrapolation to the maximum quenching $\Delta F_{max} = 0.87 \pm 0.03$ shows that, at saturation, the RSF1010 RepA hexamer binds 6.0 ± 0.3 molecules of TNP-ADP.

The determination of the maximum stoichiometry of the nucleoside triphosphate analogue, TNP-ATP, binding to the RepA hexamer has been performed in an analogous way. Fluorescence titrations of the RepA hexamer with TNP-ATP

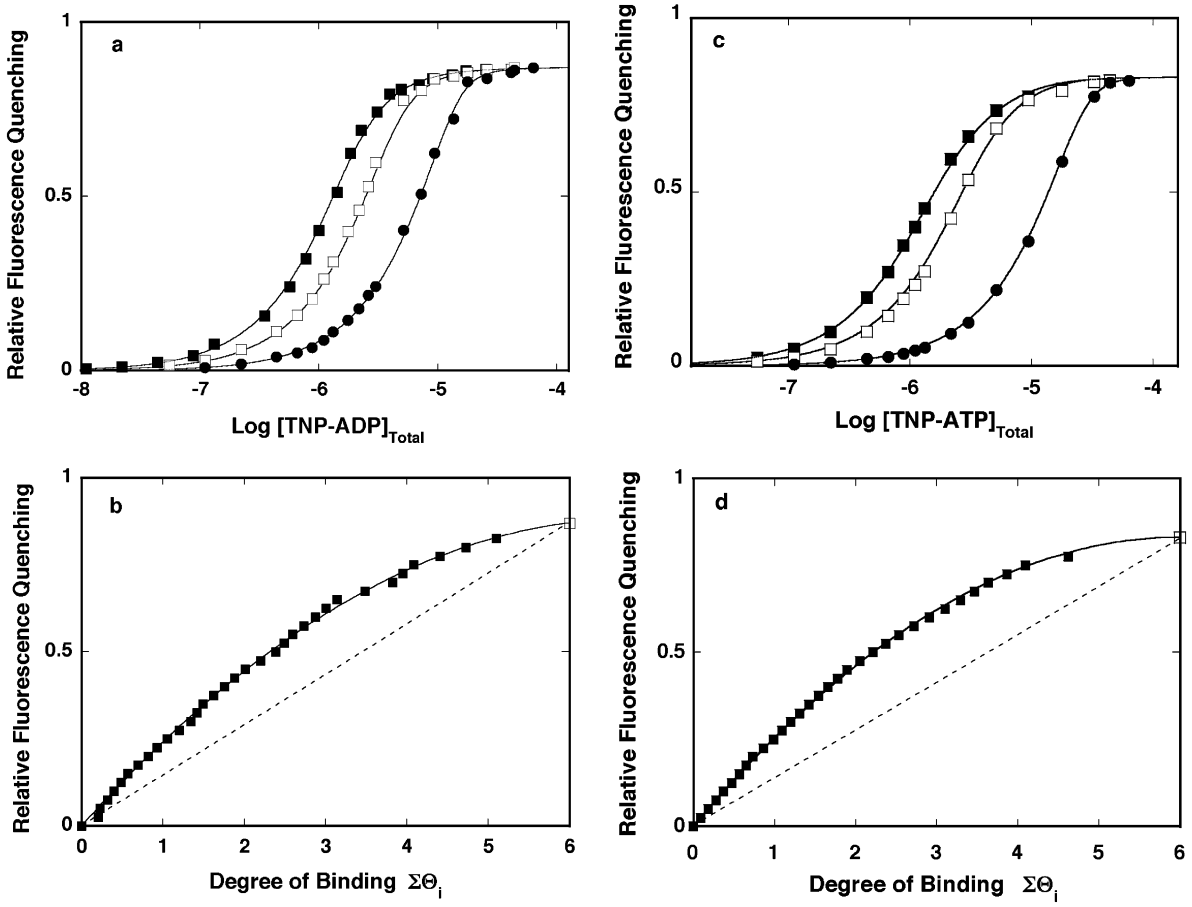

FIGURE 1: (a) Fluorescence titration of the RepA helicase with TNP-ADP in buffer T5 (at pH 7.6 and 10 °C), containing 10 mM NaCl and 1 mM $MgCl_2$, at different RepA protein concentrations (■) 5×10^{-7}, (□) 1×10^{-6}, and (●) 3×10^{-6} M (hexamer). The solid lines are nonlinear least-square fits of the titration curves, according to the hexagon model (eqs 5−8) using a single set of binding parameters with the intrinsic binding constant $K = 8.0 \times 10^6$ M^{-1} and cooperativity parameter $\sigma = 0.36$. The relative fluorescence change, ΔF_{obs}, is defined as a function of the average degree of binding by eq 8. (b) Dependence of the relative fluorescence quenching, ΔF_{obs}, upon the average degree of binding of TNP-ADP on the RepA hexamer, $\sum\Theta_i$ (■). The values of $\sum\Theta_i$ have been determined using the quantitative method described in Materials and Methods. The solid line is the nonlinear least-square fit using the second-degree polynomial function defined by eq 8. The dashed line is the hypothetical dependence of ΔF_{obs} upon $\sum\Theta_i$ that assumes a strict linear relationship between the observed fluorescence quenching and the average degree of binding. The maximum value of $\Delta F_{max} = 0.87 \pm 0.03$. (c) Fluorescence titration of the RepA helicase with TNP-ATP in buffer T5 (at pH 7.6 and 10 °C), containing 10 mM NaCl and 1 mM $MgCl_2$, at different RepA protein concentrations (■) 5×10^{-7}, (□) 1×10^{-6}, and (●) 6×10^{-6} M (hexamer). The solid lines are nonlinear least-square fits of the titration curves, according to the hexagon model (eqs 5−8) using a single set of binding parameters with the intrinsic binding constant $K = 2.38 \times 10^6$ M^{-1} and cooperativity parameter $\sigma = 0.37$. The relative fluorescence change, ΔF_{obs}, is defined as a function of the average degree of binding by eq 9. (d) Dependence of the relative fluorescence quenching, ΔF_{obs}, upon the average degree of binding of TNP-ADP on the RepA hexamer, $\sum\Theta_i$ (■). The values of $\sum\Theta_i$ have been determined using the quantitative method described in Materials and Methods. The solid line is the nonlinear least-square fit using the second-degree polynomial function defined by eq 9. The dashed line is the theoretical dependence of ΔF_{obs} upon $\sum\Theta_i$ that assumes a strict linear relationship between the observed fluorescence quenching and the average degree of binding. The maximum value of $\Delta F_{max} = 0.83 \pm 0.03$.

at three different protein concentrations are shown in Figure 1c. At saturation, the maximum quenching of the RepA helicase emission is 0.83 ± 0.03, which is similar, although not identical, to the value obtained for the RepA hexamer−TNP-ADP complex. The dependence of the protein fluorescence quenching, ΔF_{obs}, upon the average degree of binding of TNP-ATP on the RepA hexamer is shown in Figure 1d. The separation of the isotherms allows us to obtain $\sum\Theta_i$ up to ~4.6. Similar to the TNP-ADP case (Figure 1b), the plot is nonlinear, indicating that the binding of the first three cofactor molecules is accompanied by a larger quenching of the protein fluorescence than the quenching accompanying the saturation of the remaining nucleotide-binding sites. Extrapolation to the maximum value of $\Delta F_{max} = 0.83 \pm 0.03$ shows that, at saturation, 6.0 ± 0.5 TNP-ATP molecules bind to the RepA hexamer.

The maximum stoichiometry of the RepA hexamer−nucleotide complex has also been examined using an independent sedimentation velocity approach (*38*, *39*). We utilized the fact that TNP-modified analogues of ADP and ATP, with a molecular weight of ~700, have a much lower sedimentation coefficient than the RepA hexamer (MW ~ 180 000). Moreover, the nucleotide analogues have a characteristic absorption band between ~400 and 500 nm allowing us to monitor the sedimentation of the cofactor without interference of the protein absorption. Sedimentation velocity scans of TNP-ADP (monitored at 445 nm) in the presence of the RepA hexamer, in buffer T5 (at pH 7.6 and 10 °C), containing 10 mM NaCl and 1 mM $MgCl_2$, are shown in Figure 2. The concentrations of the RepA hexamer and TNP-ADP are 3×10^{-6} and 6×10^{-5} M, respectively.

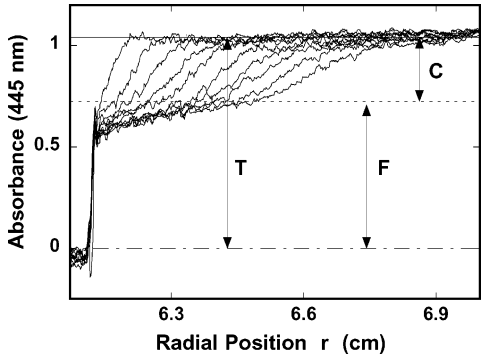

FIGURE 2: Sedimentation velocity absorption profiles at 445 nm of TNP-ADP in the presence of the RepA hexamer, in buffer T5 (at pH 7.6 and 10 °C), containing 10 mM NaCl and 1 mM $MgCl_2$. Concentrations of TNP-ADP and the RepA protein are 6.0×10^{-5} and 3×10^{-6} M (hexamer), respectively. The scans were collected at 35 000 rpm. The short initial parts of the scans correspond to the buffer−air region above the meniscus. The arrows indicate the absorption of the total concentration of TNP-ADP (*T*), the concentration of the cofactor bound in the complex with the RepA hexamer (*C*), and the concentration of the free TNP-ADP (*F*). The horizontal lines indicate the locations of the plateaus corresponding to the zero line (— - —), free TNP-ADP concentration (- - -), and total TNP-ADP concentration (—).

At selected total concentrations of the nucleotide and the helicase, $[TNP\text{-}ADP]_T$ and $[RepA]_T$, we should observe complete saturation of the RepA hexamer with the nucleotide as indicated by the data shown in parts a and b of Figure 1. The fast moving boundary in Figure 2 corresponds to the TNP-ADP−RepA hexamer complex (*38*). The slow moving boundary corresponds to the free TNP-ADP. In fact, at an applied rotational velocity of 35 000 rpm, the boundary of the free TNP-ADP barely moves from the meniscus. From the total absorption of the initial scans (*T*) that corresponds to the total TNP-ADP concentration and the absorption of the slow moving boundary (*F*), one can directly calculate the absorption of the bound TNP-ADP, as $C = T - F$. In turn, the amount of the bound cofactor to the RepA hexamer is $C[TNP\text{-}ADP]_T$. The determined average degree of binding is then $\sum\Theta_i = (C[TNP\text{-}ADP]_T)/[RepA]_T = 6.1 \pm 0.5$, indicating that six molecules of TNP-ADP are bound per RepA hexamer, in excellent agreement with the quantitative fluorescence titration data (parts a and b of Figure 1).

Heterogeneity in Macroscopic Affinities of the Nucleotide-Binding Sites of the RepA Hexamer. Because we have quantitatively determined the average degree of binding, $\sum\Theta_i$, over ∼80% of the spectroscopic titration curves, we can obtain the free nucleotide concentrations, using eq 3b, and construct a true thermodynamic binding isotherm, i.e., the average degree of binding, $\sum\Theta_i$, as a function of the free nucleotide concentration (*34*). The dependence of $\sum\Theta_i$ upon the free concentration of the $[TNP\text{-}ADP]_F$ is shown in Figure 3a. An analogous plot of $\sum\Theta_i$ as a function of $[TNP\text{-}ATP]_F$ is shown in Figure 3b. A striking feature of these plots, not affected by changes of the observed spectroscopic signal (fluorescence quenching), is that the binding isotherms extend over more than 2 orders of magnitude of the free nucleotide concentration, i.e., between ∼10 and ∼90% of the maximum degree of binding. If the six binding sites had the same affinity for the ligand (nucleotide cofactor), then the free ligand concentration cannot span more than 2 orders of magnitude between 10 and ∼90% of the maximum degree

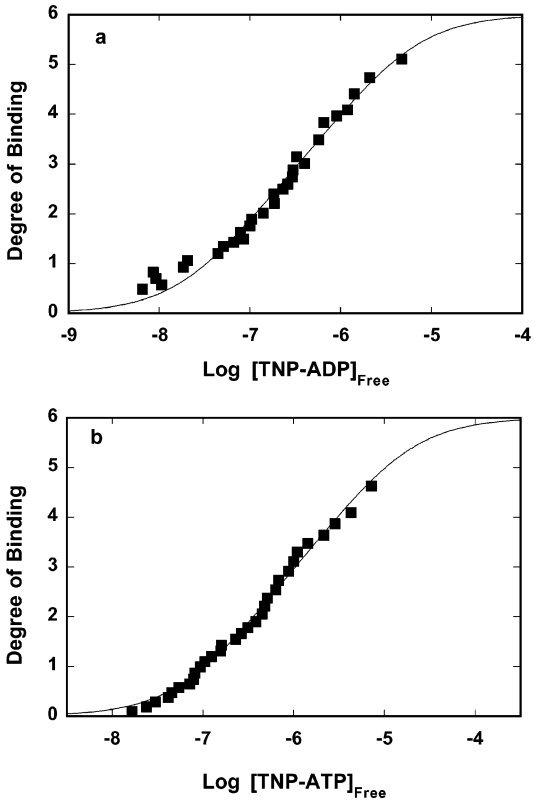

FIGURE 3: (a) Average number of TNP-ADP molecules bound per RepA hexamer as a function of the free concentration of the cofactor in buffer T5 (at pH 7.6 and 10 °C), containing 10 mM NaCl and 1 mM $MgCl_2$. The isotherm has been constructed using the quantitative method described in the Material and Methods (eqs 2 and 3) (see the text for details). The solid line is the nonlinear least-square fit according to the hexagon model (eqs 5−8) with the intrinsic binding constant $K = 7.7 \times 10^6$ M^{-1} and cooperativity parameter $\sigma = 0.38$. (b) Average number of TNP-ATP molecules bound per RepA hexamer as a function of the free concentration of the cofactor in buffer T5 (at pH 7.6 and 10 °C), containing 10 mM NaCl and 1 mM $MgCl_2$. The isotherm has been constructed using the general method described in the Material and Methods (eqs 2 and 3). The solid line is the nonlinear least-square fit according to the hexagon model (eqs 5−7) with the intrinsic binding constant $K = 2.38 \times 10^6$ M^{-1} and cooperativity parameter $\sigma = 0.4$.

of binding (*40*, *41*). In other words, a binding system of multiple discrete binding sites, without heterogeneity in their intrinsic affinities, cannot generate such behavior. Therefore, these data unambiguously show that the macroscopic affinities of the nucleotide cofactors for the RepA hexamer are a decreasing function of the degree of binding, $\sum\Theta_i$ (see the Discussion).

Statistical Thermodynamic Model for the Nucleotide Binding to the RSF1010 RepA Protein Hexamer. The crystal structure of the RepA hexamer shows that in the hexamer the protomers form a ring-like structure with the protomer−protomer contacts limited to two adjacent subunits (*14*). The thermodynamic data discussed above show that the RSF1010 RepA hexamer binds six nucleotide molecules and the binding is characterized by the decreasing macroscopic affinity with the increase of the degree of binding. The simplest statistical thermodynamic model, i.e., the model containing the smallest number of parameters that can account for such behavior is that the RepA hexamer exhibits nearest-neighbor negative cooperativity among otherwise

identical six nucleotide-binding sites. This model, referred to as the hexagon model, has been previously used to analyze binding of six nucleotides and six DnaC protein molecules to the *E. coli* DnaB hexamer (*25*, *26*, *35*, *39*). The other possible simple model of the nucleotide binding to the six sites of the RepA hexamer, also containing only two binding parameters, is that the hexamer possesses two independent classes of independent binding sites, with each class encompassing three independent binding sites. However, as we discuss below, this model does not apply to the RepA hexamer.

In the hexagon model, there are only two parameters that characterized the binding, the intrinsic binding constant, K, and the parameter, σ, describing cooperative interactions (*25*). The first ligand can bind to any of six, initially equivalent binding sites. The cooperative interactions are limited to only two neighboring sites. The partition functions for the model, Z_H, is then

$$Z_H = 1 + 6x + 3(3 + 2\sigma)x^2 + 2(1 + 6\sigma + 3\sigma^2)x^3 + 3(3\sigma^2 + 2\sigma^3)x^4 + 6\sigma^4x^5 + \sigma^6x^6 \quad (5)$$

where $x = KN_F$ and N_F is the free nucleotide concentration. The average degree of binding, $\sum\Theta_i$, is defined by the standard statistical thermodynamic formula (*40*)

$$\sum\Theta_i = \frac{\partial \ln Z_H}{\partial \ln L} \quad (6)$$

and

$$\sum\Theta_i = \frac{6x + 6(3 + 2\sigma)x^2 + 6(1 + 6\sigma + 3\sigma^2)x^3 + 12(3\sigma^2 + 2\sigma^3)x^4 + 30\sigma^4x^5 + 6\sigma^6x^6}{Z_H} \quad (7)$$

To directly analyze the spectroscopic titration curves using analytical eqs 5−7, one would have to know all molar fluorescence intensities of all possible RepA−nucleotide complexes. As pointed out above, in practice, such an approach would be a hopeless task (*25*, *35*). However, one can utilize the fact that we have determined the empirical dependence of the observed fluorescence quenching of the RepA−TNP−nucleotide system as a function of the average degree of binding of nucleotide cofactors, shown in parts b and d in Figure 1, and applied the empirical function approach, described in the Materials and Methods (*25*, *35*). In the case of TNP-ADP, the plot of the observed fluorescence quenching, ΔF_{obs}, as a function of the average degree of binding, $\sum\Theta_i$, in Figure 1b is represented by a second-degree polynomial function (eq 4) with the coefficients $a_1 = 2.6054 \times 10^1$ and $a_2 = -1.9220 \times 10^2$, respectively, as

$$\Delta F_{obs} = 2.6054 \times 10^1(\sum\Theta_i) - 1.9224 \times 10^2(\sum\Theta_i)^2 \quad (8)$$

This function is then used to fit and generate theoretical titration curves of the TNP-ADP binding to the RepA helicase, using the hexagon model, and to extract intrinsic binding constant, K, and cooperativity parameter, σ. The solid lines in Figure 1a are the nonlinear least-square fits of the experimental isotherms for TNP-ADP binding to the RepA hexamer, using eqs 5−8, with a single set of binding parameters, that provide the intrinsic binding constant $K = (8.0 \pm 1.5) \times 10^6\ M^{-1}$ and $\sigma = 0.36 \pm 0.05$. Thus, the obtained results indicate that binding of the six TNP-ADP molecules to the RepA hexamer is characterized by significant negative cooperativity (see the Discussion).

In the case of TNP-ATP, the plot of the observed fluorescence quenching, ΔF_{obs}, as a function the average degree of binding, $\sum\Theta_i$, in Figure 1d is described by a second-degree polynomial function (eq 4) as

$$\Delta F_{obs} = 2.7618 \times 10^1(\sum\Theta_i) - 2.2957 \times 10^2(\sum\Theta_i)^2 \quad (9)$$

The solid lines in Figure 1c are the nonlinear least-square fits of the experimental isotherms for TNP-ATP binding to the RepA hexamer, using eqs 5−8, with a single set of binding parameters, that provide the intrinsic binding constant $K = (2.4 \pm 0.3) \times 10^6\ M^{-1}$ and $\sigma = 0.40 \pm 0.05$. It is evident that, similar to the TNP-ADP, the binding of six TNP-ATP molecules to the RepA hexamer is characterized by significant negative cooperativity (see the Discussion).

The empirical function method, as described above, provides the most accurate approach to determine the binding parameters by allowing the fit of the entire spectroscopic titration curve (*25*, *35*). On the other hand, the availability of the thermodynamic isotherms, i.e., the dependence of the degree of binding upon the free nucleotide cofactor concentration over ~80% of the total saturation, shown in parts a and b of Figure 3, gives an opportunity to obtain the values of the intrinsic binding constants, K, and cooperativity parameter, σ, independently of any consideration of the applied spectroscopic signal. The solid lines in parts a and b of Figure 3 are the nonlinear least-square fits of the thermodynamic isotherms for TNP-ADP and TNP-ATP binding the RepA hexamer, according to the hexagon model, with only two binding parameters, using eqs 5−8. The obtained values of the intrinsic binding constants and cooperativity parameters are $K = (7.7 \pm 1.5) \times 10^6\ M^{-1}$ and $\sigma = 0.38 \pm 0.05$ and $K = (2.4 \pm 0.2) \times 10^6\ M^{-1}$ and $\sigma = 0.37 \pm 0.05$, for TNP-ADP and TNP-ATP, respectively. Thus, as expected, both the empirical function approach and the thermodynamic isotherm analyses provide, within experimental accuracy, the same values of the intrinsic binding parameters for the ADP and ATP analogues to the RepA hexamer (see the Discussion).

Binding of MANT-ADP to the RepA Hexamer. To test the effect of the chemical modification on the general aspects of the nucleotide cofactor binding to the RepA hexamer, such as maximum stoichiometry and the cooperative nature of the binding process, we performed analogous fluorescence titrations and analyses for the binding of a different fluorescent ADP analogue, MANT-ADP, to RepA helicase. As in the case of TNP derivatives, this nucleotide analogue is also modified on the ribose (*31*). Moreover, similar to TNP-modified nucleotides, the absorption spectrum of the MANT moiety overlaps with the emission spectrum of the RepA protein, indicating that binding of the cofactor, if in close proximity of the protein tryptophans, should induce a significant quenching of the protein emission (*25*). Fluorescence titrations of RepA helicase with MANT-ADP in buffer T5 (at pH 8.1 and 10 °C), containing 10 mM NaCl and 1 mM $MgCl_2$, at two different protein concentrations are shown

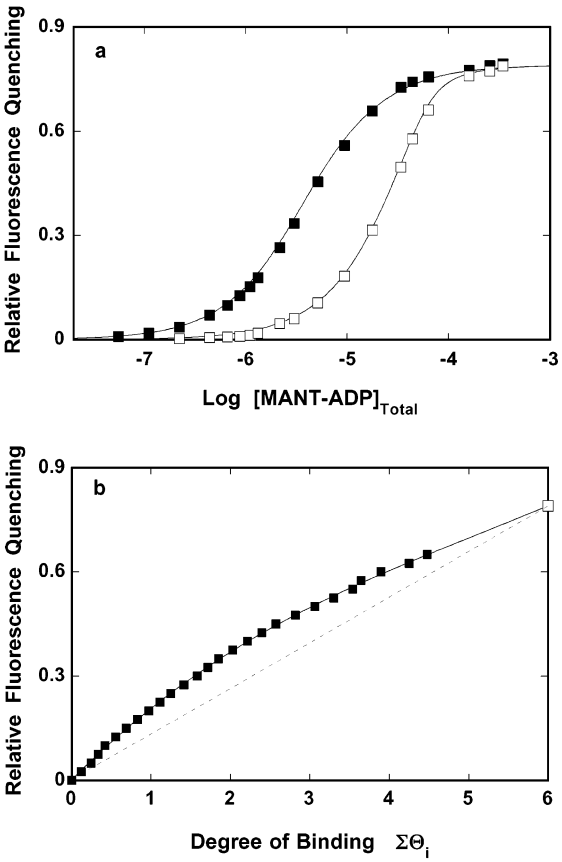

FIGURE 4: (a) Fluorescence titration of the RepA helicase with MANT-ADP in buffer T5 (at pH 7.6 and 10 °C), containing 10 mM NaCl and 1 mM $MgCl_2$, at different RepA protein concentrations 1×10^{-6} (■) and 1×10^{-5} M (hexamer) (□). The solid lines are nonlinear least-square fits of the titration curves, according to the hexagon model (eqs 5−8) using a single set of binding parameters with the intrinsic binding constant $K = 5 \times 10^5$ M^{-1}, cooperativity parameter $\sigma = 0.65$, and the third-degree polynomial, empirical function (eq 2) (see b). (b) Dependence of the relative fluorescence quenching, ΔF_{obs}, upon the average degree of binding of MANT-ADP on the RepA hexamer, $\sum\Theta_i$ (■). The values of $\sum\Theta_i$ have been determined using the quantitative method described in Materials and Methods. The solid line is the nonlinear least-square fit using the third-degree polynomial function (eq 2) with the coefficients $a_1 = 2.3210 \times 10^{-1}$, $a_2 = -2.7528 \times 10^{-2}$, and $a_3 = 1.7991 \times 10^{-3}$. The dashed line is the theoretical dependence of ΔF_{obs} upon $\sum\Theta_i$ that assumes a strict linear relationship between the observed fluorescence quenching and the average degree of binding. The maximum value of $\Delta F_{max} = 0.79 \pm 0.03$.

in Figure 4a. Binding of the MANT-modified cofactor to the RepA hexamer is accompanied by a strong quenching of the RepA protein fluorescence with the maximum quenching, at saturation, $\Delta F_{max} = 0.79 \pm 0.03$, very similar to the values obtained for TNP-modified cofactors. However, the titration curves are shifted toward a higher nucleotide concentration range, indicating that the macroscopic affinity of the MANT-ADP is significantly lower than the affinity of the TNT-modified analogues (parts a and c of Figure 1).

The dependence of the observed fluorescence quenching, ΔF_{obs}, upon the average degree of binding, $\sum\Theta_i$, of MANT-ADP on the RepA hexamer is shown in Figure 4b. At the selected protein concentrations, the separation of the binding isotherms allows us to obtain the values of $\sum\Theta_i$ up to ~4.5 of the MANT-ADP molecules per the RepA hexamer. Extrapolation to the maximum quenching $\Delta F_{max} = 0.79 \pm 0.03$ shows that, at saturation, the RSF1010 RepA hexamer binds 6 ± 0.5 molecules of MANT-ADP. As observed in the case of TNP-modified cofactors, the plot in Figure 4b is clearly nonlinear and can be accurately described by an empirical function, in this case a third-degree polynomial (eq 2), with the coefficients $a_1 = 2.3210 \times 10^{-1}$, $a_2 = -2.7528 \times 10^{-2}$, and $a_3 = 1.7991 \times 10^{-3}$. The solid lines in Figure 4a are the nonlinear least-square fits of the experimental isotherms of the MANT-ADP binding to the RepA hexamer, using the determined empirical function and eqs 5−8, with a single set of binding parameters, that provide the intrinsic binding constant $K = (5.0 \pm 0.7) \times 10^5$ M^{-1} and $\sigma = 0.65 \pm 0.12$. Thus, as observed in the case of TNP-ADP and TNP-ATP, the binding of the six MANT-ADP molecules to the RepA hexamer is characterized by a negative cooperativity (see the Discussion).

DISCUSSION

At Saturation, the RepA Hexamer Binds Six Nucleotide Cofactors. The maximum stoichiometry of the RepA−nucleotide complex has been determined in direct binding experiments with fluorescent nucleotide analogues, TNP-ADP, TNP-ATP, and MANT-ADP. Competition studies with unmodified nucleotides, described in the accompanying paper 2, show that the analogues strictly bind to the nucleotide-binding site of the helicase (*27*). The thermodynamic studies have been greatly facilitated by the finding that the association of the nucleotide analogues with the RepA helicase is accompanied by a strong quenching of the fluorescence of the enzyme (*17*). A similar strong quenching of the protein emission has been previously found in the case of the *E. coli* DnaB hexameric helicase and was extensively used by us to quantitatively examine the structure, thermodynamics, and kinetics of the DnaB helicase interactions with the nucleotide cofactors (*25*, *26*, *35*, *39*) (see below).

In our studies, we could determine the average degree of binding, $\sum\Theta_i$, of the TNP-ADP up to ~5.1 cofactor molecules per RepA hexamer. Short extrapolation to the maximum value of the observed fluorescence quenching, ΔF_{max}, provides the maximum value of $\sum\Theta_i = 6.0 \pm 0.3$ (Figure 1b). The same value of the maximum stoichiometry has been obtained in experiments with the triphosphate analogue, TNP-ATP (Figure 1d). Independent analysis, using the sedimentation velocity technique, shows that six TNP-ADP molecules are associated with the RepA hexamer that contains a saturating concentration of the nucleotide (Figure 2). Thus, we have established that, at saturation, the RepA hexamer binds six molecules of nucleotide cofactors. In other words, the RepA hexamer has six nucleotide-binding sites, and each site can engage in interactions with the nucleotide cofactor molecule. In this aspect, the RepA hexamer behaves exactly like the *E. coli* DnaB helicase, transcription termination factor Rho, and SV40 T large antigen helicases (*25*, *26*, *35*, *39*, *43*−*45*). However, this behavior is very different from the bacteriophage T7 hexameric helicase, where only binding of three nucleotide molecules to this homohexamer was observed in filter-binding experiments (*46*).

Binding of the Nucleotide Cofactors to the RepA Hexamer Is Characterized by Negative Cooperative Interactions Between the Adjacent Subunits. A characteristic feature of the nucleotide binding to the RepA hexamer is the decreasing macroscopic affinity of the cofactor with the increasing

degree of binding (parts a and b of Figure 3). As we discussed above, the simplest statistical thermodynamic model that can account for such behavior is the hexagon model (eqs 5−8). Each binding site is initially independent and characterized by the intrinsic binding constant, *K*. However, when the cofactor molecules are bound to two adjacent sites, they engage in cooperative interactions characterized by the cooperativity factor, σ (*25*).

A very important feature of the hexagon model is the fact that it does not make any specific prediction about the spectroscopic properties of various RepA−nucleotide entities, with different numbers of bound nucleotide cofactors, as a function of the partial spectroscopic parameters characterizing each binding site. This feature results from the fact that the presence of the cooperative interactions removes additivity in the energetics and, particularly, structural properties of a macromolecule−ligand complex. In other words, this property fundamentally differentiates the hexagon model, with cooperative interactions, from the model of two independent classes of independent binding sites, as we discussed below. It may seem that such a property of the hexagon model makes the analyses of the binding process more difficult. However, when both thermodynamic isotherms and spectroscopic titration curves are available, as obtained in this work (Figures 1 and 3), the entire complex behavior of the observed spectroscopic parameter (fluorescence quenching) can simply be defined by an empirical function (eq 2).

In the examined solution conditions, the value of the parameter characterizing cooperative interactions between bound nucleotide cofactors, σ, is 0.36 ± 0.05 and 0.38 ± 0.07 for the TNP-ADP and TNP-ATP analogue, respectively, indicating that saturation of two neighboring sites leads to the same decrease of the affinity of the nucleotide, independently of the number of phosphate groups. However, as discussed in the accompanying paper 2, this is not generally the case, and the cooperative interactions between the nucleotide-binding sites of the RepA hexamer are strongly affected by the magnesium concentration in solution, particularly, in the case of the ADP analogue. It should be noted that similar values of the cooperativity parameter, σ, have been found for the interactions of the same nucleotide analogues with the DnaB hexamer (*25*). Such similar energetics strongly suggests a similar mechanism of the intersite interactions for these two analogous hexameric helicases.

The Model of Two Independent Classes of Independent Binding Sites Does Not Describe the Nucleotide Cofactor Binding to the RepA Hexamer. As mentioned above, the alternative simple model of the nucleotide binding to the RepA hexamer that could account for the stoichiometry of six nucleotide-binding sites and the decreasing macroscopic affinity of the nucleotide binding is a model of two independent classes of independent binding sites (*17*, *40*). The partition function for this model, Z_{TC}, is then (*40*)

$$Z_{TC} = (1 + K_1 N_F)^3 (1 + K_2 N_F)^3 \qquad (10)$$

where K_1 and K_2 are the intrinsic binding constants characterizing affinities of the nucleotide cofactors in the first and second binding class, respectively. Thus, similar to the hexagon model, there are also only two binding parameters that characterize the examined interactions. The average degree of binding, $\sum\Theta_i$, is then defined as

$$\sum\Theta_i = \frac{3K_1 N_F}{(1 + K_1 N_F)} + \frac{3K_2 N_F}{(1 + K_2 N_F)} \qquad (11)$$

Recall, the major premise of this model is that the two different classes of binding sites are independent and the binding sites within each class are independent. Therefore, nucleotide binding to these two classes of sites is characterized by only two different fluorescence quenching parameters, ΔF_1 and ΔF_2, corresponding to the quenching of the protein emission in the nucleotide binding to the first and second class of the binding sites, respectively. The observed fluorescence quenching, ΔF_{obs}, at any titration point is then defined by

$$\Delta F_{obs} = \frac{\Delta F_1 K_1 N_F}{1 + K_1 N_F} + \frac{\Delta F_2 K_2 N_F}{1 + K_2 N_F} \qquad (12)$$

Therefore, unlike the hexagon model with cooperative interactions, the model with two independent classes of binding sites imposes a strict relationship between the observed spectroscopic property of different hexamer−nucleotide complexes, ΔF_{obs}, and the partial spectroscopic properties of the single binding site within each class, ΔF_1 and ΔF_2.

If only spectroscopic titration curves were available, then differentiation between the hexagon model and the model of the two independent classes of binding sites would be practically impossible. However, we can utilize the fact that we can obtain the intrinsic binding constants, K_1 and K_2, directly and independently from the spectroscopic parameters, using the thermodynamic isotherms, i.e., the dependence of the average degree of binding, $\sum\Theta_i$, as a function of the free nucleotide concentration. Fitting the isotherm in Figure 3a, according to the model of two independent classes of independent binding sites, as defined by eqs 10−12, provides $K_1 = (1.3 \pm 0.2) \times 10^7\ M^{-1}$, $K_2 = (6.6 \pm 0.6) \times 10^5\ M^{-1}$ (see the Supporting Information). Having K_1 and K_2, we can now obtain the fluorescence parameters, ΔF_1 and ΔF_2, characterizing the TNP-ADP binding to two independent classes of binding sites, as defined by eq 12. Because $\Delta F_{max} = \Delta F_1 + \Delta F_2$, and $\Delta F_{max} = 0.88$, only one quenching parameter, e.g., ΔF_2, is an independent variable. However, these values of ΔF_1 and ΔF_2 provide a much worse representation of the experimentally obtained dependence of the ΔF_{obs} upon $\sum\Theta_i$ (Figure 1b) (see the Supporting Information). These data are the first indication that the model of two independent classes of binding sites provides a worse representation of the experimental data, as compared to the hexagon model (see below).

As pointed out above, the model of the two independent classes of independent binding sites imposes a strict requirement of the additivity of the observed signal in the enzyme complexes with different numbers of the bound nucleotide cofactors, as defined by eq 12. To further examine this aspect of the behavior of the model, we performed computer simulations of the observed signal, ΔF_{obs}, as a function of the average degree of binding, $\sum\Theta_i$, for different values of the partial quenching parameters, ΔF_1 and ΔF_2, and for the cases where the values of the two binding constants,

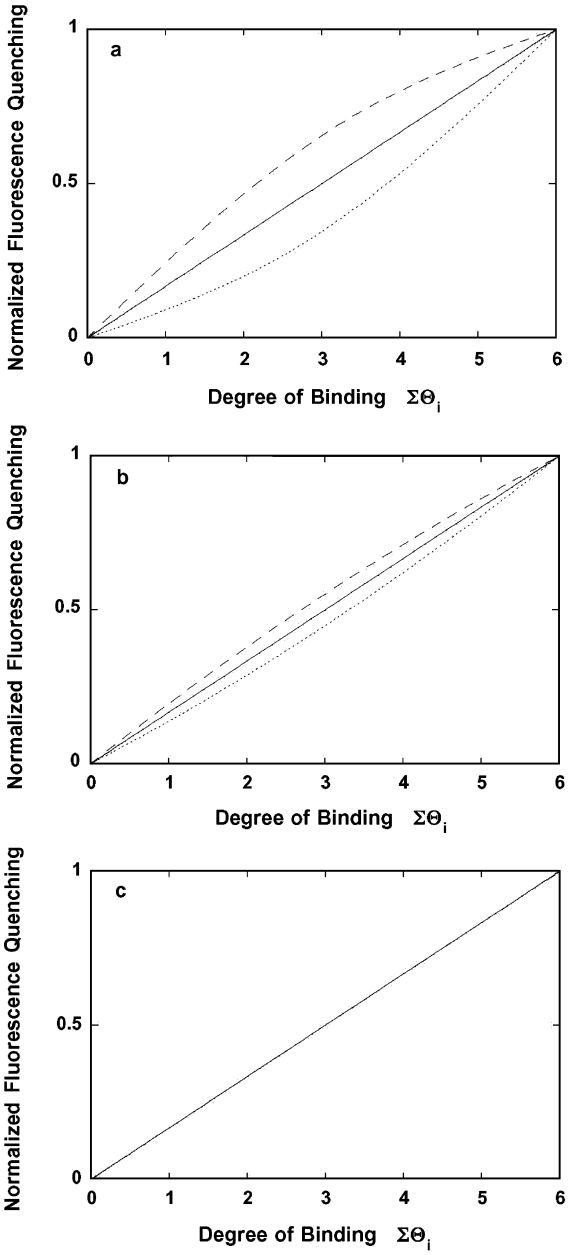

FIGURE 5: Computer simulations of the normalized fluorescence quenching, ΔF_{obs}, as a function of the average degree of binding of ligand molecules on the hexamer, $\sum\Theta_i$, for the model of the two independent classes of independent binding sites with different values of the intrinsic binding constants and partial quenching parameters, characterizing the ligand binding to each class (eqs 10−12). (a) Intrinsic binding constants, $K_1 = 1 \times 10^6$ and $K_2 = 1 \times 10^5$ M^{-1} and the quenching parameters, $\Delta F_1 = 0.8$ and $\Delta F_2 = 0.2$ (- - -), $\Delta F_1 = 0.5$ and $\Delta F_2 = 0.5$ (—), and $\Delta F_1 = 0.2$ and $\Delta F_2 = 0.8$ (···). (b) Intrinsic binding constants, $K_1 = 2 \times 10^5$and $K_2 = 1 \times 10^5$ M^{-1} and the quenching parameters, $\Delta F_1 = 0.8$ and $\Delta F_2 = 0.2$ (- - -), $\Delta F_1 = 0.5$ and $\Delta F_2 = 0.5$ (—), and $\Delta F_1 = 0.2$ and $\Delta F_2 = 0.8$ (···). (c) Intrinsic binding constants, $K_1 = 1 \times 10^5$ and $K_2 = 1 \times 10^5$ M^{-1} and the quenching parameters, $\Delta F_1 = 0.8$ and $\Delta F_2 = 0.2$ (—). The plot for $\Delta F_1 = 0.5$ and $\Delta F_2 = 0.5$ and $\Delta F_1 = 0.2$ and $\Delta F_2 = 0.8$, are included in c. However, the plots, obtained for any values of the partial quenching parameters, ΔF_1 and ΔF_2, are superimposable with the straight line shown in the c.

characterizing the two independent classes, are different or the same. The plot of ΔF_{obs}, defined by eq 12, as a function of $\sum\Theta_i$, is shown in Figure 5a. The selected values of K_1 and K_2 are 1×10^6 and 1×10^5 M^{-1}, respectively. For the cases where $\Delta F_1 < \Delta F_2$, $\Delta F_1 = \Delta F_2$, and $\Delta F_1 > \Delta F_2$, the plot is concave down, a straight line, or concave up (Figure 5a). Analogous plots for the same values of the partial quenching constants, ΔF_1 and ΔF_2, but with the binding constants $K_1 = 2 \times 10^5$ M^{-1} and $K_2 = 1 \times 10^5$ M^{-1}, i.e., differing only by a factor of 2, are shown in Figure 5b. The functional dependence of ΔF_{obs} upon $\sum\Theta_i$ is similar to that observed in Figure 5a, although, the nonlinear behavior of the plots is now much less pronounced.

On the other hand, a very different situation is observed when the two binding constants have the same values. For such case, the plot of ΔF_{obs} as a function of $\sum\Theta_i$ is shown in Figure 5c. The selected values of K_1 and K_2 are 1×10^5 and 1×10^5 M^{-1}, respectively, and the partial spectroscopic parameters are the same as in parts a and b of Figure 5. It is evident that when the binding constants, characterizing the affinity for the binding sites within each class of binding sites, have the same values, the model of the two independent classes of independent binding sites can only generate the dependence of the ΔF_{obs} upon $\sum\Theta_i$ that is a straight line, independent of the values of the partial spectroscopic parameters, ΔF_1 and ΔF_2. In other words, when binding constants K_1 and K_2 have the same values, any nonlinear dependence of ΔF_{obs} as a function of $\sum\Theta_i$ excludes the model of the two independent classes of the independent binding sites.

Such a dramatic inadequacy of the model of the two independent classes of the independent binding sites occurs in the nucleotide cofactor binding to the RepA hexamer in the absence of magnesium (accompanying paper 2). The dependence of the average degree of binding, $\sum\Theta_i$, as a function of $[TNP\text{-}ADP]_{free}$, for the titrations performed in buffer T5 (at pH 7.6 and 10 °C), containing 10 mM NaCl and in the absence of magnesium, is shown in Figure 6a. The solid line is the nonlinear least-square fit of the isotherm according to the model of two independent classes of independent binding sites (eqs 10−12) that provides $K_1 = (6.0 \pm 0.7) \times 10^4$ M^{-1} and $K_2 = (6.0 \pm 0.7) \times 10^4$ M^{-1}, respectively. Thus, in the case of TNP-ADP, in the absence of magnesium, both binding constants, characterizing two classes of binding sites, have the same value (accompanying paper 2). The dependence of the observed fluorescence quenching, ΔF_{obs}, as a function of the degree of binding, $\sum\Theta_i$, is shown in Figure 6b. The solid line is the theoretical dependence of the ΔF_{obs} upon $\sum\Theta_i$, using the hexagon model and empirical function representation of the fluorescence quenching (accompanying paper 2). The hexagon model provides an excellent description of the experimental data. The dashed line is the dependence of ΔF_{obs} upon $\sum\Theta_i$, obtained using the obtained values of the binding constants and any values of the quenching parameters, ΔF_1 and ΔF_2, as long as $\Delta F_{max} = \Delta F_1 + \Delta F_2$. In fact, as discussed above (Figure 5c), there is not a set of values of ΔF_1 and ΔF_2 that can describe the nonlinear dependence of ΔF_{obs} upon $\sum\Theta_i$ when $K_1 = K_2$. In other words, these results exclude the model of two independent classes of independent binding sites for the nucleotide binding to the RepA hexamer.

The discussed results and analyses clearly show that the model of two independent classes of independent binding sites cannot describe both the binding isotherms and the dependence of the observed quenching as a function of the degree of binding, for the nucleotide cofactor association with the RepA hexamer. The reason for this inadequacy is clearly

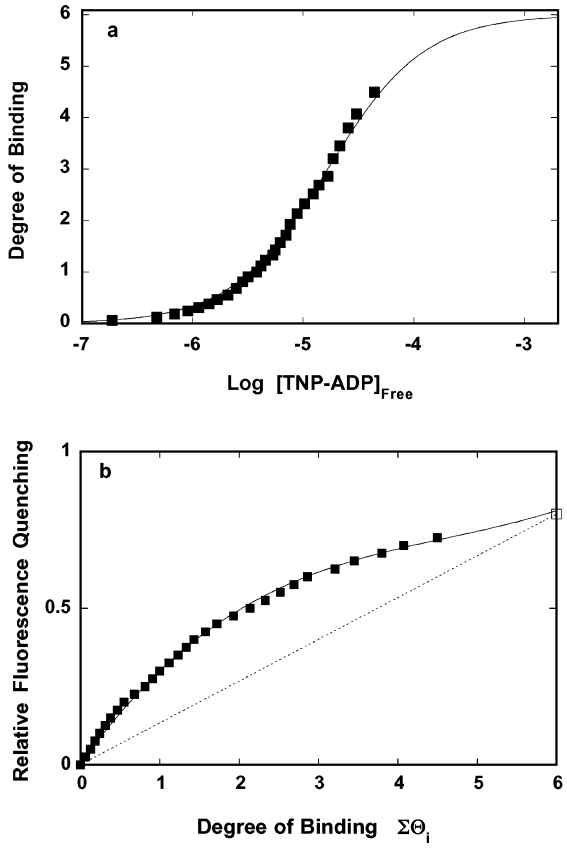

FIGURE 6: (a) Average number of TNP-ADP molecules bound per RepA hexamer as a function of the free concentration of the cofactor in buffer T5 (at pH 7.6 and 10 °C), containing 10 mM NaCl and no magnesium (accompanying paper 2). The solid line is the nonlinear least-square fit according to the model of two independent classes of independent binding sites (eqs 10−12) with the intrinsic binding constants $K_1 = 6.02 \times 10^4$ and $K_2 = 6.02 \times 10^4$ M^{-1}. (b) Dependence of the relative fluorescence quenching, ΔF_{obs}, upon the average degree of binding of TNP-ADP on the RepA hexamer, $\sum\Theta_i$ (■) in buffer T5 (at pH 7.6 and 10 °C), containing 10 mM NaCl and no magnesium. The values of $\sum\Theta_i$ have been determined using the quantitative method described in the Materials and Methods. The solid line is the nonlinear least-square fit of the experimental curve, according to the hexagon model (eqs 5−8), using as empirical function the third-degree polynomial, $\Delta F_{obs} = 0.359\,41(\sum\Theta_i) - 0.065\,685(\sum\Theta_i)^2 + 0.004\,719\,7(\sum\Theta_i)^3$ (accompanying paper 2). The dashed line is the dependence of ΔF_{obs} upon $\sum\Theta_i$ that is obtained for the model of two independent classes of independent binding sites, independent of any values of the partial quenching parameters, characterizing the TNP-ADP binding to the RepA hexamer in the examined solution conditions. The maximum value of $\Delta F_{max} = 0.80 \pm 0.03$ (accompanying paper 2).

indicated by eq 12. For the model of two independent classes of binding sites to describe both the isotherm and the observed spectroscopic signal (in our case, fluorescence quenching), the partial molar spectroscopic parameters must be additive in all complexes of the ligand with the macromolecule. This is the main requirement of this model, if the classes of binding sites and the sites are supposed to be independent. The binding of the nucleotide cofactors to the RepA hexamer, evidently, does not fulfill this requirement. In other words, *the partial quenching parameters characterizing different RepA hexamer−nucleotide complexes are not simple additive functions of the quenching parameters characterizing single binding sites*. In this context, as pointed out above, the hexagon model is not limited by any strict requirement for the additivity of the partial spectroscopic parameters. The partial fluorescence intensities are specific for a particular RepA−nucleotide complex; i.e., interactions of a cofactor molecule with a particular site are affected by what happens at the neighboring sites. The behavior is very complex and requires the analysis using the empirical function method (see above) (*25*, *35*). Such behavior provides direct evidence of cooperative interactions between the nucleotide-binding sites of the RepA hexamer (see accompanying paper 2). Moreover, in general, finding even a single set of conditions where the observed spectroscopic parameter, affected by multiple ligand binding to a macromolecule, is not a simple additive function of spectroscopic parameters, characterizing particular binding sites, constitutes a proof that the binding sites are not independent.

The binding of the nucleotide cofactors to the RepA helicase has been examined before, although those studies have been limited to a semiquantitative examination of the observed quenching of the protein fluorescence induced by the analogue of ADP, ϵADP (*17*). The analysis was based on the "fluorescence quenching factor", an approach that assumes strict proportionality between the observed signal and the average degree of binding which, in general, as discussed above, does not apply to such complex binding systems (*25*, *34*, *37*). The maximum stoichiometry of the RepA hexamer−ϵADP complex was not determined but assumed on the basis of the homohexameric crystal structure of the protein. However, bacteriophage T7 hexameric helicase also possesses six presumed nucleotide-binding sites, yet only binding of three nucleotide molecules to the hexamer was detected (*46*). The observed fluorescence quenching was then analyzed by assuming a model of two independent classes of binding sites. As we discussed above, such a model does not apply to the nucleotide binding to the RepA hexamer and the obtained binding parameters are affected by the differences in the quenching parameters induced upon the nucleotide binding to different sites. Nevertheless, the obtained data suggested heterogeneity of the nucleotide-binding sites of the enzyme, in agreement with the quantitative analyses described here.

Still, little is known about the role of the negative cooperativity in nucleotide binding to a hexameric helicase. This role may be related to the fact that the enzyme is a multisubunit protein involved *in vivo* in multiple processes where nucleotide binding and/or hydrolysis plays a regulatory role (*2*). For instance, a common feature of the interactions of the replicative hexameric helicase with the ssDNA is that the affinity of the protein for the nucleic acid is strongly increased in the presence of ATP analogues, but in the presence of ADP, the affinity is diminished (*9*, *17*−*24*). Also, in the case of the DnaB hexamer, formation of the specific DnaB−ssDNA complex, recognized by primase, requires ATP as a positive effector but is inhibited by ADP (*47*). Negative cooperative interactions introduce structural and functional differentiation among otherwise identical subunits of the multisubunit enzyme (accompanying paper 2). Thus, large global conformational changes of the DnaB hexamer, induced by nucleotide binding to the enzyme, have already been documented, both by hydrodynamic and electron microscopy methods (*38*, *48*, *49*). Whether or not RepA hexamer undergoes similar global conformational changes is not yet known.

Notice that, unlike the model of the two classes of binding sites, where the functional difference between subunits is preprogrammed before the nucleotide binding, the model with the cooperative interactions does not impose such preprogramming. Rather, the population of different forms of the hexamer is controlled by the nucleotide concentration, with each subunit capable of being a strong or weak binding site. Such functional asymmetry may enable the helicase to hydrolyze ATP to ADP by one set of subunits while still preserving strong affinity for the ssDNA at another subunit (accompanying paper 2). This mechanism must be operational in the unwinding reaction of the duplex DNA where the helicase cycles between high and low affinity for the ssDNA with concomitant hydrolysis of ATP (*2*−*4*). Thus, the functional heterogeneity among different sets of nucleotide-binding sites, resulting from cooperative interactions among them, would be crucial for the catalytic cycle of the unwinding reaction.

Strong Quenching of the Protein Tryptophan Fluorescence Indicates That the Tryptophans Are in Close Proximity to the Nucleotide-Binding Sites. Strong, ~80%, quenching of the tryptophan emission of the RepA helicase is not without precedence. Binding of the same fluorescent derivatives of nucleotide cofactors to the six nucleotide-binding sites of the *E. coli* DnaB hexameric helicase is accompanied by a similar, ~70%, quenching of the protein fluorescence (*25*). Although the crystal structure of the DnaB helicase is still unknown, spectroscopic studies indicated that the tryptophan residues are clustered in a localized region of the protein. Moreover, the data indicate that the tryptophans form a hydrophobic pocket around the nucleotide-binding site of the enzyme (*50*). The observed strong quenching of the DnaB protein emission by the TNP and MANT derivative of nucleotide cofactors predominantly result from a very efficient fluorescence energy transfer from the protein tryptophans to the TNP and MANT moieties of the analogues.

In the crystal structure of the RepA hexamer, three of four tryptophan residues of the protein are located in a close vicinity to the Walker sequence, a conserved motif of a presumed nucleotide-binding site (*51*). Such similarity of the tryptophans' location in the surrounding of the nucleotide-binding site of both hexameric helicases is striking and suggests a role of these aromatic residues in the functioning of the site. However, whether the tryptophan residues of the RepA helicase are a part of the nucleotide hydrophobic pocket is still not known. Nevertheless, it is rather certain that the main origin of the strong quenching of the RepA protein fluorescence is the same as observed in the case of the DnaB helicase, i.e., an efficient fluorescence energy transfer from the tryptophans to the TNP and MANT groups, because of the close proximity of both chromophores with strongly overlapping emission and absorption bands (*41*, *50*). On the other hand, the fact that the quenching is not identical for TNP-ADP and TNP-ATP indicates the conformational changes induced by the nucleotide binding also contribute to the observed fluorescence quenching and that these conformational changes are not identical for the di- and triphosphate nucleotides. Our laboratory is currently examining these aspects of the RepA hexamer−nucleotide cofactor interactions.

ACKNOWLEDGMENT

We thank Betty Sordahl for reading the manuscript.

SUPPORTING INFORMATION AVAILABLE

Figure showing (a) plot of $\sum\Theta_i$ as a function of $[TNP\text{-}ADP]_{free}$, (b) fluorescence titration curves of the RepA hexamer with TNP-ADP fitted with the obtained binding constants and with the optimal values of $\Delta F_1 = 0.750$ and $\Delta F_2 = 0.129$, and (c) observed fluorescence quenching, ΔF_{obs}, as a function of the degree of binding, $\sum\Theta_i$. This material is available free of charge via the Internet at http://pubs.acs.org.

REFERENCES

1. Kornberg, A., and Baker, T. A. (1992) *DNA Replication*, pp 275−306, Freeman, San Francisco, CA.
2. Lohman, T. M., and Bjornson, K. P. (1996) Mechanisms of helicase-catalyzed DNA unwinding, *Annu. Rev. Biochem. 65*, 169−214.
3. von Hippel, P. H., and Delagoutte, E. (2002) Helicase mechanisms and the coupling of helicases within macromolecular machines. Part I: Structures and properties of isolated helicases, *Q. Rev. Biophys. 35*, 431−478.
4. von Hippel, P. H., and Delagoutte, E. (2003) Helicase mechanisms and the coupling of helicases within macromolecular machines. Part II: Integration of helicases into cellular processes, *Q. Rev. Biophys. 36*, 1−69.
5. Bujalowski, W., Klonowska, M. M., and Jezewska, M. J. (1994) Oligomeric structure of *Escherichia coli* primary replicative helicase DnaB protein, *J. Biol. Chem. 269*, 31350−31358.
6. Jezewska, M. J., Rajendran, S., and Bujalowski, W. (1998) Complex of *Escherichia coli* primary replicative helicase DnaB protein with a replication fork. Recognition and structure, *Biochemistry 37*, 3116−3136.
7. Egelman, E. H., Yu, X., Wild, R., Hingorani, M. M., and Patel, S. S. (1995) Bacteriophage T7 helicase/primase proteins form rings around single-stranded DNA that suggest a general structure for hexameric helicases, *Proc. Natl. Acad. Sci. U.S.A. 92*, 3869−3873.
8. Dong, F., Gogol, E. P., and von Hippel, P. H. (1995) The phage T4-coded DNA replication helicase (gp41) forms a hexamer upon activation by nucleoside triphosphate, *J. Biol. Chem. 270*, 7462−7473.
9. Patel, S. S., and Picha, K. M. (2000) Structure and function of hexameric helicases, *Annu. Rev. Biochem. 69*, 651−697.
10. De Gaaf, J., Crossa, J., H., Heffron, F., and Falkow, S. (1978) Replication of the nonconjugative plasmid RSF1010 in *Escherichia coli* K-12, *J. Bacteriol. 134*, 1117−1122.
11. Guerry, P., van Embden, J., and Falkow, S. (1974) Molecular nature of two nonconjugative plasmids carrying drug resistance genes, *J. Bacteriol. 117*, 987−997.
12. Scherzinger, E., Ziegelin, G., Barcena, M., Carazo, J. M., Lurz, R., and Lanka, E. (1997) The RepA protein of plasmid RSF1010 is a replicative DNA helicase, *J. Biol. Chem. 272*, 30228−30236.
13. Roleke, D., Hoier, H., Bartsch, C., Umbach, P., Scherzinger, E., Lurz, R., and Saenger, W. (1997) Crystallization and preliminary crystallographic and electron microscopy study of bacterial DNA helicase (RSF1010 RepA), *Acta Crystallogr., Sect. D 53*, 213−216.
14. Niedenzu, T., Roleke, D., Bains, Scherzinger, E., and Saenger, W. (2001) Crystal structure of the hexameric helicase RepA of plasmid RSF1010, *J. Mol. Biol. 306*, 479−487.
15. Xu, H., Frank, J., Holzwarth, J. F., Saenger, W., and Behlke, J. (2000) Interaction of different oligomeric states of hexameric DNA−helicase RepA with single-stranded DNA studied by analytical ultracentrifugation, *FEBS Lett. 482*, 180−184.
16. Xu, H., Frank, J., Trier, U., Hammer, S., Schroder, W., Behlke, J., Schafer-Korting, M., Holzwarth, J. F., and Saenger, W. (2001) Interactions of fluorescence labeled single-stranded DNA with hexameric DNA−helicase RepA: A photon and fluorescence correlation spectroscopy studies, *Biochemistry 40*, 7211−7218.
17. Xu, H., Frank, J., Niedenzu, T., and Seanger, W. (2000) DNA helicase RepA: Cooperative ATPase activity and binding of nucleotides, *Biochemistry 39*, 12225−12233.

18. Bujalowski, W., and Jezewska, M. J. (1995) Interactions of *Escherichia coli* primary replicative helicase DnaB protein with single-stranded DNA. The nucleic acid does not wrap around the protein hexamer, *Biochemistry 34*, 8513−8519.
19. Jezewska, M. J., Kim, U.-S., and Bujalowski, W. (1996) Binding of *Escherichia coli* primary replicative helicase DnaB protein to single-stranded DNA. Long-range allosteric conformational changes within the protein hexamer, *Biochemistry 35*, 2129−2145.
20. Bujalowski, W., Klonowska, M. M., and Jezewska, M. J. (1994) Oligomeric structure of *Escherichia coli* primary replicative helicase DnaB protein, *J. Biol. Chem. 269*, 31350−31358.
21. Jezewska, M. J., and Bujalowski, W. (1996) A general method of analysis of ligand binding to competing macromolecules using the spectroscopic signal originating from a reference macromolecule. Application to *Escherichia coli* replicative helicase DnaB protein−nucleic acid interactions, *Biochemistry 35*, 2117−2128.
22. Jezewska, M. J., Rajendran, S., and Bujalowski, W. (1997) Strand specificity in the interactions of *Escherichia coli* primary replicative helicase DnaB protein with replication fork, *Biochemistry 36*, 10320−10326.
23. Jezewska, M. J., Rajendran S., Bujalowska, D., and Bujalowski, W. (1998) Does ssDNA pass through the inner channel of the protein hexamer in the complex with the *E. coli* DnaB helicase? Fluorescence energy transfer studies, *J. Biol. Chem. 273*, 10515−10529.
24. Jezewska, M. J., Rajendran, S., and Bujalowski, W. (1998) Complex of *Escherichia coli* primary replicative helicase DnaB protein with a replication fork. Recognition and structure, *Biochemistry 37*, 3116−3136.
25. Bujalowski, W., and Klonowska, M. M. (1993) Negative cooperativity in the binding of nucleotides to *Escherichia coli* replicative helicase DnaB protein. Interactions with fluorescent nucleotide analogs, *Biochemistry 32*, 5888−5900.
26. Jezewska, M. J., Kim, U.-S., and Bujalowski, W. (1996) Interactions of *Escherichia coli* primary replicative helicase DnaB protein with nucleotide cofactors, *Biophys. J. 71*, 2075−2086.
27. Bujalowski, W., and Jezewska, M. J. (2000) Kinetic mechanism of the single-stranded DNA recognition by *Escherichia coli* replicative helicase DnaB protein. Application of the matrix projection operator technique to analyze stopped-flow kinetics, *J. Mol. Biol. 295*, 831−852.
28. Rajendran, S., Jezewska, M. J., and Bujalowski W. (2000) Multiple-step kinetic mechanism of DNA-independent ATP binding and hydrolysis by *Escherichia coli* replicative helicase DnaB protein: Quantitative analysis using the rapid quench-flow method, *J. Mol. Biol. 303*, 773−795.
29. Edelhoch, H. (1967) Spectroscopic determination of tryptophan and tyrosine in proteins, *Biochemistry 6*, 1948−1954.
30. Gill, S. C., and von Hippel, P. H. (1989) Calculation of protein extinction coefficients from amino acid sequence data, *Anal. Biochem. 182*, 319−326.
31. Hiratsuka, T. (1983) New ribose-modified fluorescent analogs of adenine and guanine nucleotides available as substrates for various enzymes, *Biochim. Biophys. Acta 742*, 496−508.
32. Lakowicz, J. R. (1999) *Principles of Fluorescence Spectroscopy*, pp 25−61, Plenum Press, New York.
33. Azumi, T., and McGlynn, S. P. (1962) Polarization of the luminescence of phenantrene, *J. Chem. Phys. 37*, 2413−2420.
34. Lohman, T. M., and Bujalowski, W. (1991) Thermodynamic methods for model-independent determination of equilibrium binding isotherms for protein−DNA interactions: Spectroscopic approaches to monitor binding, *Methods Enzymol. 208*, 258−290.
35. Jezewska, M. J., and Bujalowski, W. (1997) Quantitative analysis of ligand−macromolecule interactions using differential quenching of the ligand fluorescence to monitor the binding, *Biophys. Chem. 64*, 253−269.
36. Jezewska, M. J., Galletto, R., and Bujalowski, W. (2004) Interactions of the RepA helicase hexamer of plasmid RSF1010 with the ssDNA. Quantitative analysis of stoichiometries, intrinsic affinities, cooperativities, and heterogeneity of the total ssDNA-binding site, *J. Mol. Biol. 343*, 115−136.
37. Bujalowski, W., and Jezewska, M. J. (2000) *Spectrophotometry and Spectrofluorimetry. A Practical Approach* (Gore, M. G., Ed.) pp 141−165, Oxford University Press, New York.
38. Galletto, R., Jezewska, M. J., and Bujalowski, W. (2003) Interactions of the *Escherichia coli* DnaB helicase hexamer with the replication factor the DnaC protein. Effect of nucleotide cofactors and the ssDNA on protein−protein interactions and the topology of the complex, *J. Mol. Biol. 329*, 441−465.
39. Jezewska, M. J., and Bujalowski, W. (1996) Global conformational transitions in *E. coli* primary replicative DnaB protein induced by ATP, ADP, and single-stranded DNA binding, *J. Biol. Chem. 271*, 4261−4265.
40. Hill, T. L. (1985) *Cooperativity Theory in Biochemistry. Steady State and Equilibrium Systems*, pp 167−234, Springer-Verlag, New York.
41. Cantor, R. C., and Schimmel, P. R. (1980) *Biophysical Chemistry*, Vol. III, pp 849−886, W. H. Freeman, New York.
42. Bujalowski, W., and Klonowska, M. M. (1994) Structural characteristics of the nucleotide binding site of the *E. coli* primary replicative helicase DnaB protein. Studies with ribose and base-modified fluorescent nucleotide analogs, *Biochemistry 33*, 4682−4694.
43. Geiselmann, J., and von Hippel, P. H. (1992) Functional interactions of ligand cofactors with *Escherichia coli* trascription termination factor Rho. I. Binding of ATP, *Protein Sci. 1*, 850−860.
44. Geiselmann, J., Yager, T. D., and von Hippel, P. H. (1992) Functional interactions of ligand cofactors with *Escherichia coli* trascription termination factor Rho. II. Binding of RNA, *Protein Sci. 1*, 861−873.
45. Huang, S.-G., Weisshart, K., and Fanning, E. (1998) Characterization of the nucleotide binding properties of SV40 T antigen using fluorescent 3′(2′)-*O*-(2,4,6-trinitrophenyl)adenine nucleotide analogs, *Biochemistry 37*, 15336−15344.
46. Hingorani, M. M., and Patel, S. S. (1996) Cooperative interactions of nucleotide ligands are linked to oligomerization and DNA binding in bacteriophage T7 gene 4 helicases, *Biochemistry 35*, 2218−2228.
47. Arai, K., and Kornberg, A. (1981) Mechanism of DnaB protein action. Allosteric role of ATP in the alteration of DNA structure by DnaB protein in priming replication, *J. Biol. Chem. 256*, 5260−5266.
48. Egelman, E. H., Yu, X., Wild, R., Hingorani, M. M., and Patel, S. S. (1995) Bacteriophage T7 helicase/primase proteins form rings around single-stranded DNA that suggest a general structure for hexameric helicases, *Proc. Natl. Acad. Sci. U.S.A. 92*, 3869−3873.
49. Yang, S., Yu., X., VanLoock, M. S., Jezewska, M. J., Bujalowski, W., and Egelman, E. H. (2002) Flexibility of the rings: Structural asymmetry in the DnaB hexameric helicase, *J. Mol. Biol. 321*, 839−849.
50. Bujalowski, W., and Klonowska, M. M. (1994) Close proximity of tryptophan residues and ATP-binding site in *Escherichia coli* primary replicative helicase DnaB protein. Molecular topography of the enzyme, *J. Biol. Chem. 269*, 31359−31371.
51. Walker, J. E., Saraste, M., Runswick, M. J., and Gray, N. J. (1982) Distantly related sequences in the α- and β-subunits of ATP synbthase, myosin, kinases, and other ATP-requiring enzymes and a common nucleotide binding fold, *EMBO J. 1*, 945−951.

BI048037+